Johann Radon Institute for
Computational and Applied Mathematics
Austrian Academy of Sciences (ÖAW)

Functional type error control for stabilised space-time IgA approximations to parabolic problems

U. Langer, S. Matculevich, S. Repin

RICAM-Report 2017-14

Functional type error control for stabilised space-time IgA approximations to parabolic problems

Ulrich Langer*, Svetlana Matculevich*, and Sergey Repin**

*RICAM Linz, Johann Radon Institute, Linz, Austria
{smatculevich,ulanger}@ricam.oeaw.ac.at
**St. Petersburg Department of V.A. Steklov Institute of Mathematics RAS; University of Jyvaskyla, Finland
sergey.s.repin@jyu.fi,serepin@pdmi.ras.ru

Abstract. The paper is concerned with reliable space-time IgA schemes for parabolic initial-boundary value problems. We deduce a posteriori error estimates, and investigate their applicability to space-time IgA approximations. Since the derivation is based on purely functional arguments, the estimates do not contain mesh dependent constants, and are valid for any approximation from the admissible (energy) class. In particular, they imply estimates for discrete norms associated with stabilised space-time IgA approximations. Finally, we illustrate the reliability and efficiency of presented error estimates for the approximate solutions recovered with IgA techniques on a model example.

Key words: Error control, functional error estimates, stabilised space-time IgA schemes, fully-adaptive space-time schemes

Countless usage of the time-dependent systems governed by parabolic partial differential equations (PDEs) in scientific and engineering applications trigger their active investigation in mathematical and numerical modelling. By virtue of the fast development of parallel computers, treating time in the evolutionary equations as yet another dimension in space became quite natural. The *space-time approach* is not restricted with the disadvantages of time-marching schemes. On the contrary, it becomes quite useful when efficient parallel methods and their implementation on massively parallel computers are considered (see, e.g., [7,21]).

Investigation of effective adaptive refinement methods is crucial for the construction of fast and efficient solvers for PDEs. In the same time, the aspect of scheme localisation is strongly linked with reliable and quantitatively efficient a posteriori error estimation tools. The latter one is expected to identify the areas of the considered computational domain with relatively high discretisation errors, and provide the fully automated refinement strategy in order to reach the desired accuracy level for the current reconstruction. Local refinement tools of IgA (e.g., T-splines, THB-splines, and LR-splines) have been combined with various a posteriori error estimation techniques, e.g., error estimates using the hierarchical bases [4,32], residual-based [10,33,2,15], and goal-oriented error estimates [31,3,16,17]. Below, we use a different (functional) method providing fully guaranteed error estimates in the various weighted norms equivalent to the global energy norm. These estimates include only global constants (independent of the mesh characteristic h), and are valid for any approximation from the admissible functional space. Functional error estimates (so-called majorants and minorants of the derivation from the exact solution) were introduced in [28,29] and later applied to different mathematical models [26,22] . They provide guaranteed, sharp, and fully computable upper and lower bounds of errors. This approach in combination with IgA approximations generated by tensor-product splines was investigated in [13] for elliptic boundary value problems (BVP).

In this paper, we derive functional-type a posteriori error estimates for time-dependent problems (cf. also [27]) in the context of the space-time IgA scheme introduced in [21]. The latter one exploits the time-upwind test function motivated by the space-time streamline diffusion method (see, e.g., [9,11,12]) and approximations provided by IgA framework. By exploiting the universality and efficiency of the considered error estimates as well as the smoothness of the IgA approximations, we aim at the construction of fully-adaptive, fast and efficient parallel space-time methods that could tackle complicated problems inspired by industrial applications.

This work has the following structure: Section 1 defines the problem and discusses its solvability, whereas Section 2 presents the stabilised space-time IgA scheme with its main properties. An overview of main ideas and definitions used in the IgA framework can be found in the same section. In Section 3, we introduce new functional type a posteriori error estimates using the stabilised formulation of parabolic initial BVPs (I-BVPs). Finally, Section 4 presents numerical results demonstrating the efficiency of the majorants in the elliptic case.

1 Model Problem

Let $\overline{Q} := Q \cup \partial Q$, $Q := \Omega \times (0,T)$, denote the space-time cylinder, where $\Omega \subset \mathbb{R}^d$, $d \in \{1,2,3\}$, is a bounded Lipschitz domain with boundary $\partial\Omega$, and $(0,T)$ is a given time interval, $0 < T < +\infty$. Here, the cylindrical surface is defined as $\partial Q := \Sigma \cup \overline{\Sigma}_0 \cup \overline{\Sigma}_T$ with $\Sigma = \partial\Omega \times (0,T)$, $\Sigma_0 = \Omega \times \{0\}$, and $\Sigma_T = \Omega \times \{T\}$. We discuss our approach to guaranteed error control of space-time approximations with the paradigm of the classical *linear parabolic I-BVP*: find $u : \overline{Q} \to \mathbb{R}$ satisfying the system

$$\partial_t u - \Delta_x u = f \quad \text{in} \quad Q, \qquad u = 0 \quad \text{on} \quad \Sigma, \qquad u = u_0 \quad \text{on} \quad \overline{\Sigma}_0, \tag{1}$$

where ∂_t is the time derivative, Δ_x denotes the Laplace operator in space, $f \in L^2(Q)$, and $u_0 \in H^1_0(\Sigma_0)$ are the given source function and initial data, respectively. Here, $L^2(Q)$ is the space of square-integrable functions over Q quipped with the usual norm and scalar product denoted respectively by $\| v \|_Q := \| v \|_{L^2(Q)}$ and $(v,w)_Q := \int_Q v(x,t)w(x,t)\,\mathrm{d}x\mathrm{d}t$, $\forall v, w \in L^2(Q)$.

By $H^k(Q)$, $k \geq 1$, we denote spaces of functions having generalised square-summable derivatives of the order k with respect to (w.r.t.) space and time. Next, we introduce the Sobolev spaces

$$\begin{aligned} H^1_0(Q) &:= \big\{u \in H^1(Q) : u|_\Sigma = 0\big\},\\ H^1_{0,\overline{0}}(Q) &:= \big\{u \in H^1_0(Q) : u_{\Sigma_T} = 0\big\},\\ V_0 := H^1_{0,\underline{0}}(Q) &:= \big\{u \in H^1_0(Q) : u_{\Sigma_0} = 0\big\}, \quad \text{and}\\ V_0^{\Delta_x} := H_0^{\Delta_x,1}(Q) &:= \big\{u \in H^1_0(Q) \,:\, \Delta_x u \in L^2(Q)\big\}. \end{aligned}$$

Moreover, we use auxiliary Hilbert spaces for vector-valued functions

$$\begin{aligned} H^{\mathrm{div}_x,0}(Q) &:= \big\{\boldsymbol{y} \in [L^2(Q)]^d \,:\, \mathrm{div}_x \boldsymbol{y} \in L^2(Q)\big\} \quad \text{and}\\ H^{\mathrm{div}_x,1}(Q) &:= \big\{\boldsymbol{y} \in H^{\mathrm{div}_x,0}(Q) \,:\, \partial_t \boldsymbol{y} \in [L^2(Q)]^d\big\} \end{aligned}$$

equipped with respective norm and semi-norm

$$\|\boldsymbol{y}\|^2_{H^{\mathrm{div}_x,0}} := \|\mathrm{div}_x\, \boldsymbol{y}\|^2_Q \qquad \text{and} \quad \|\boldsymbol{y}\|^2_{H^{\mathrm{div}_x,1}} := \|\mathrm{div}_x\, \boldsymbol{y}\|^2_Q + \|\partial_t\, \boldsymbol{y}\|^2_Q.$$

In what follows, C_{F} stands for the constant in the Friedrichs inequality

$$\|w\|_Q \leq C_{\mathrm{F}} \|\nabla_x w\|_Q, \quad \forall w \in H^{1,0}_0(Q) := \big\{u \in L^2(Q) : \nabla_x u \in [L^2(Q)]^2, u|_\Sigma = 0\big\}.$$

From [19] it follows that, if $f \in L^2(Q)$ and $u_0 \in H^1_0(\Sigma_0)$, the problem (1) is uniquely solvable in $V_0^{\Delta_x}$, and the solution u depends continuously on t in the $H^1_0(\Omega)$-norm. Moreover, according to [19, Remark 2.2], $\| \nabla_x u(\cdot,t) \|^2_\Omega$ is an absolutely continuous function of $t \in [0,T]$ for any $u \in V_0^{\Delta_x}$. If $u_0 \in L^2(\Sigma_0)$, then the problem has a unique solution u in even wider class $H^{1,0}_0(Q)$, and it satisfies the generalised formulation of (1)

$$(\nabla_x u, \nabla_x w)_Q - (u, \partial_t w)_Q =: a(u,w) = l(w) := (f,w)_Q + (u_0, w)_{\Sigma_0} \tag{2}$$

for all $w \in H^1_{0,\overline{0}}(Q)$, where $(u_0,w)_{\Sigma_0} := \int_{\Sigma_0} u_0(x)\, w(x,0)dx = \int_\Omega u_0(x)\, w(x,0)dx$. However, according to the well-established arguments (see [18,19,34]), without loss of generality, we homogenise the problem, i.e., consider (2) with $u_0 = 0$.

Our main goal is to derive fully computable estimates for space-time IgA approximations of this class of problems. For this purpose, we use the functional approach to a posteriori error estimates. Initially, their simplest form has been obtained for a heat equation in [27]. Numerical properties of above-mentioned error estimates w.r.t. the time-marching and space-time method are discussed in [6,25,24].

2 Stabilised formulation of the problem and its discretization

For the convenience of the reader, we first recall the general concept of the IgA approach, the definition of B-splines (NURBS) and their use in the geometrical representation of the space-time cylinder Q, as well as in the construction of the IgA trial spaces, which are used to approximate solutions satisfying the variational formulation (2).

Let $p \geq 2$ denote a degree of polynomials used for the IgA approximations and n denote a number of basis functions used to construct a B-spline curve. A *Knot-vector* in $\mathbb{R}$ is a non-decreasing set of coordinates in a parameter domain, written as $\Xi = \{\xi_1, ..., \xi_{n+p+1}\}$, $\xi_i \in \mathbb{R}$, where $\xi_1 = 0$ and $\xi_{n+p+1} = 1$. The knots can be repeated, and the multiplicity of the i-th knot is indicated by m_i. Throughout the paper, we consider only open knot vectors, i.e., $m_1 = m_{n+p+1} = p+1$. For a one-dimensional parametric domain $\widehat{Q} := (0,1)$, $\widehat{\mathcal{K}}_h := \{\widehat{K}\}$ denotes a locally quasi-uniform mesh, where each element $\widehat{K} \in \widehat{\mathcal{K}}_h$ is constructed by the distinct neighbouring knots. The global size of $\widehat{\mathcal{K}}_h$ is denoted by $\hat{h} := \max_{\widehat{K}\in\widehat{\mathcal{K}}_h}\{\hat{h}_{\widehat{K}}\}$, where $\hat{h}_{\widehat{K}} := \mathrm{diam}(\widehat{K})$.

The *univariate B-spline basis functions* $\widehat{B}_{i,p} : \widehat{Q} \to \mathbb{R}$ are defined by means of Cox-de Boor recursion formula

$$\widehat{B}_{i,p}(\xi) := \tfrac{\xi-\xi_i}{\xi_{i+p}-\xi_i}\,\widehat{B}_{i,p-1}(\xi) + \tfrac{\xi_{i+p+1}-\xi}{\xi_{i+p+1}-\xi_{i+1}}\widehat{B}_{i+1,p-1}(\xi), \quad \widehat{B}_{i,0}(\xi) := \begin{cases} 1 & \text{if} \quad \xi_i \leq \xi \leq \xi_{i+1} \\ 0 & \text{otherwise} \end{cases}, \tag{3}$$

and are $(p-m_i)$-times continuously differentiable across the i-th knot with multiplicity m_i. It is important to note that the scope of this paper is limited to a single-patch domain. The *multivariate B-splines* on the parameter domain $\widehat{Q} := (0,1)^{d+1}$, $d = \{1,2,3\}$, is defined as a tensor-product of the corresponding univariate ones. In multidimensional case, we define the knot-vector dependent on the coordinate direction $\Xi^\alpha = \{\xi_1^\alpha, ..., \xi_{n^\alpha+p^\alpha+1}^\alpha\}$, $\xi_i^\alpha \in \mathbb{R}$, where $\alpha = 1, ..., d+1$ indicates the direction (in space or time). Furthermore, we introduce set of multi-indices $\mathcal{I} = \big\{\, i = (i_1, ..., i_{d+1}) : i_\alpha = 1, ..., n_\alpha,\ \alpha = 1, ..., d+1 \big\}$ and multi-index $p := (p_1, ..., p_{d+1})$ indicating the order of polynomials. The tensor-product of the univariate B-spline basis functions generates multivariate B-spline basis functions $\widehat{B}_{i,p}(\boldsymbol{\xi}) := \prod_{\alpha=1}^{d+1}\widehat{B}_{i_\alpha,p_\alpha}(\xi^\alpha)$, where $\boldsymbol{\xi} = (\xi^1, ..., \xi^{d+1}) \in \widehat{Q}$. The *univariate and multivariate NURBS basis* functions are defined in the parametric domain by means of B-spine basis functions, i.e., for given p and any $i \in \mathcal{I}$ $\widehat{R}_{i,p} : \widehat{Q} \to \mathbb{R}$ is defined as $\widehat{R}_{i,p}(\boldsymbol{\xi}) := \frac{w_i\,\widehat{B}_{i,p}(\boldsymbol{\xi})}{W(\boldsymbol{\xi})}$. Here, $W(\boldsymbol{\xi})$ is a weighting function $W(\boldsymbol{\xi}) := \sum_{i\in\mathcal{I}} w_i\,\widehat{B}_{i,p}(\boldsymbol{\xi})$, where $w_i \in \mathbb{R}^+$.

The physical space-time domain $Q \subset \mathbb{R}^{d+1}$ is defined by the geometrical mapping of the parametric domain $\widehat{Q} := (0,1)^{d+1}$:

$$\Phi : \widehat{Q} \to Q := \Phi(\widehat{Q}) \subset \mathbb{R}^{d+1}, \quad \Phi(\boldsymbol{\xi}) := \sum_{i\in\mathcal{I}} \widehat{R}_{i,p}(\boldsymbol{\xi})\,\mathbf{P}_i, \tag{4}$$

where $\{\mathbf{P}_i\}_{i\in\mathcal{I}} \in \mathbb{R}^{d+1}$ are the control points. For simplicity, we assume the same polynomial degree for all coordinate directions, i.e., $p_\alpha = p$ for all $\alpha = 1, ..., d+1$. By means of geometrical mapping (4), the mesh $\mathcal{K}_h$ discretising Q is defined as $\mathcal{K}_h := \big\{K = \Phi(\widehat{K}) : \widehat{K} \in \widehat{\mathcal{K}}_h\big\}$. The global mesh size is denoted by

$$h := \max_{K\in\mathcal{K}_h}\{\, h_K \,\}, \quad h_K := \|\nabla\Phi\|_{L^\infty(K)}\hat{h}_{\widehat{K}}. \tag{5}$$

Moreover, we assume that $\mathcal{K}_h$ is quasi-uniform mesh, i.e., there exists a positive constant C_u independent of h, such that $h_K \leq h \leq C_u\,h_K$.

The finite dimensional spaces on Q are constructed by a push-forward of the NURBS basis functions $V_h := \mathrm{span}\big\{\phi_{h,i} := \widehat{R}_{i,p} \circ \Phi^{-1}\big\}_{i\in\mathcal{I}}$, where the geometrical mapping Φ is invertible in Q, with smooth inverse on each element $K \in \mathcal{K}_h$ (see [30,1]). The subspace $V_{0h} := V_h \cap V_{0,\underline{0}}^{\Delta_x}(Q)$, where $V_{0,\underline{0}}^{\Delta_x} := V_0 \cap H_{0,\underline{0}}^{\Delta_x,1}(Q)$ is introduced for the functions satisfying homogeneous boundary condition (BC).

Stable space-time IgA scheme for (1) has been presented and analysed in [21], where the authors proved its efficiency for fixed and moving spatial computational domains. In our analysis, we use spline-bases of sufficiently high order, so that $v_h \in V_{0h} \subset V_{0,\underline{0}}$. In order to provide efficient discretization method, we test (1) with the time-upwind test-function

$$\lambda\,w + \mu\,\partial_t w, \quad w \in V_{0,\underline{0}}^{\nabla_x\partial_t} := \{w \in V_{0,\underline{0}}^{\Delta_x} : \nabla_x\partial_t w \in L^2(Q)\}, \quad \lambda, \mu \geq 0. \tag{6}$$

and arrive at the stabilised weak formulation for $u \in V_0$, i.e.,

$$\big(\partial_t u, \lambda\,w + \mu\,\partial_t w\big)_Q + \big(\nabla_x u, \nabla_x(\lambda\,w + \mu\,\partial_t w)\big)_Q =: a_s(u,w) = l_s(w) := (f, \lambda\,w + \mu\,\partial_t w)_Q, \quad \forall w \in V_{0,\underline{0}}^{\nabla_x\partial_t}. \tag{7}$$

In [21], it was shown that *stable discrete IgA space-time scheme* corresponds to the case, when $\lambda = 1$ and $\mu = \delta_h = \theta h$ in (6) with $\theta > 0$ and global mesh-size h (cf. (5)). Hence, (7) implies the discrete stabilised space-time problem: find $u_h \in V_{0h}$ satisfying

$$(\partial_t u_h, v_h + \delta_h\partial_t v_h)_Q + \big(\nabla_x u_h, \nabla_x(v_h + \delta_h\partial_t v_h)\big)_Q =: a_{s,h}(u_h, v_h) = l_{s,h}(v_h) := (f, v_h + \delta_h\,\partial_t v_h)_Q, \quad \forall v_h \in V_{0h}. \tag{8}$$

The V_{0h}-coercivity of $a_h(\cdot,\cdot) : V_{0h} \times V_{0h} \to \mathbb{R}$ w.r.t. the norm

$$|\!|\!| v_h |\!|\!|^2_{s,h} := \|\nabla_x v_h\|^2_Q + \delta_h \|\partial_t v_h\|^2_Q + \|v_h\|^2_{\Sigma_T} + \delta_h \|\nabla_x v_h\|^2_{\Sigma_T} \tag{9}$$

follows from [21, Lemma 1]. Moreover, following [21,20] one can show a boundedness property of the bilinear form $a_{h,s}(\cdot,\cdot)$ in appropriately chosen norms. Combining these coercivity and boundedness properties of $a_{h,s}(\cdot,\cdot)$ with the consistency of the scheme (8) and approximation results for the IgA spaces implies an corresponding a priori error estimate presented in Theorem 1 below.

Theorem 1. *Let $u \in H^s_0(Q) := H^s(Q) \cap H^{1,0}_0(Q)$, $s \in \mathbb{N}$, $s \geq 2$, be the exact solution of (2) and $u_h \in V_{0h}$ be the solution of (8) with some fixed parameter θ. Then, the following a priori error estimate*

$$\|u - u_h\|_{s,h} \leq C\, h^{r-1} \|u\|_{H^r(Q)} \tag{10}$$

holds, where $r = \min\{s, p+1\}$, $C > 0$ is a generic constant independent of h.

Proof: See, e.g., [21, Theorem 8]. □

3 Error majorant

In this section, we derive error majorants of the functional type for stabilised weak formulation of parabolic I-BVPs. They provide guaranteed and fully computable upper bounds of the distance between from v to the exact solution u. The functional nature of these majorants allows to obtain a posteriori error estimates for $u \in V^{\Delta_x}_{0,\underline{0}}$ and any conforming $v \in V^{\Delta_x}_{0,\underline{0}}$. The error $e = u - v$ is measured in terms of

$$|\!|\!| e |\!|\!|^2_{s,\nu_i} := \nu_1 \|\nabla_x e\|^2_Q + \nu_2 \|\partial_t e\|^2_Q + \nu_3 \|\nabla_x e\|^2_{\Sigma_T} + \nu_4 \|e\|^2_{\Sigma_T}, \tag{11}$$

where $\{\nu_i\}_{i=1,\dots,4}$ are the positive weights introduced in the derivation process.

To obtain guaranteed error bounds of $|\!|\!| e |\!|\!|^2_{s,\nu_i}$, we apply a method similar to the one developed in [27,25] for parabolic I-BVPs. For the derivation process, we consider space of smoother functions $V^{\nabla_x \partial_t}_{0,\underline{0}}$ (cf. (6)) equipped with the norm

$$\|w\|_{V^{\nabla_x \partial_t}_{0,\underline{0}}} := \sup_{t \in [0,T]} \|\nabla_x w(\cdot,t)\|^2_Q + \|w\|^2_{V^{\Delta_x}_{0,\underline{0}}},$$

where $\|w\|^2_{V^{\Delta_x}_{0,\underline{0}}} := \|\Delta_x w\|^2_Q + \|\partial_t w\|^2_Q$, which is dense in $V^{\Delta_x}_{0,\underline{0}}$. According to [19, Remark 2.2], norms $\|\cdot\|_{V^{\nabla_x \partial_t}_{0,\underline{0}}} \approx \|\cdot\|_{V^{\Delta_x}_{0,\underline{0}}}$.

Let $u_n \in V^{\nabla_x \partial_t}_{0,\underline{0}}$ and substitute it into the identity (7), i.e.,

$$a_s(u_n, w) = (f_n, \lambda\, w + \mu\, \partial_t w)_Q, \quad \text{where} \quad f_n = (u_n)_t - \Delta_x u_n \in L^2(Q). \tag{12}$$

By subtracting $a_s(v_n, w)$, $v_n \in V^{\nabla_x \partial_t}_{0,\underline{0}}$, from the LHS and RHS of (12), and by setting $w = e_n = u_n - v_n \in V^{\nabla_x \partial_t}_{0,\underline{0}}$, we arrive at the so-called 'error-identity'

$$\begin{aligned} &\lambda \|\nabla_x e_n\|^2_Q + \mu \|\partial_t e_n\|^2_Q + \tfrac{1}{2}\,(\mu \|\nabla_x e_n\|^2_{\Sigma_T} + \lambda \|e_n\|^2_{\Sigma_T}) \\ &\qquad = \lambda\Big((f_n - \partial_t v_n, e_n)_Q - (\nabla_x v_n, \nabla_x e_n)_Q\Big) + \mu\Big((f_n - \partial_t v_n, \partial_t e_n)_Q - (\nabla_x v_n, \nabla_x\, \partial_t e_n)_Q\Big), \end{aligned}$$

which is used in the derivation of the majorants of (11) in Theorems 2 and 3.

Theorem 2. *For any $v \in V^{\Delta_x}_{0,\underline{0}}$ and $\boldsymbol{y} \in H^{\mathrm{div}_x,0}(Q)$, the following estimate holds:*

$$\begin{aligned} |\!|\!| e |\!|\!|^2_{s,\nu_i} \leq \overline{\mathrm{M}}(v, \boldsymbol{y}; \gamma, \alpha_i) := \gamma\Big\{ &\lambda\big((1+\alpha_1) \|\mathbf{r}_{\mathrm{d}}\|^2_Q \\ &+ (1 + \tfrac{1}{\alpha_1})\, C^2_{\mathrm{F}} \|\mathbf{r}_{\mathrm{eq}}\|^2_Q\big) + \mu\big((1+\alpha_2) \|\mathrm{div}_x \mathbf{r}_{\mathrm{d}}\|^2_Q + (1 + \tfrac{1}{\alpha_2}) \|\mathbf{r}_{\mathrm{eq}}\|^2_Q\big)\Big\}, \end{aligned} \tag{13}$$

where $\nu_1 = (2 - \frac{1}{\gamma})\,\lambda$, $\nu_2 = (2 - \frac{1}{\gamma})\,\mu$, $\nu_3 = \mu$, $\nu_4 = \lambda$, C_{F} is the Friedrichs constant, $\mathbf{r}_{\mathrm{eq}}$ and $\mathbf{r}_{\mathrm{d}}$ are residual functionals defined by relations

$$\mathbf{r}_{\mathrm{eq}}(v, \boldsymbol{y}) := f - \partial_t v + \mathrm{div}_x\, \boldsymbol{y} \quad \textit{and} \quad \mathbf{r}_{\mathrm{d}}(v, \boldsymbol{y}) := \boldsymbol{y} - \nabla_x v, \tag{14}$$

$\lambda, \mu > 0$ are weights introduced in (6), $\gamma \in [\frac{1}{2}, +\infty)$, and $\alpha_i > 0, i = 1, 2$.

Proof: The right-hand side (RHS) of the error-identity is modified by means of the relation $(\mathrm{div}_x \boldsymbol{y}, \lambda\, e_n + \mu\, \partial_t e_n)_Q + (\boldsymbol{y}, \nabla_x(\lambda\, e_n + \mu\, \partial_t e_n))_Q = 0$. The obtained result can be presented as follows:

$$\lambda\, \|\nabla_x e_n\|_Q^2 + \mu\, \|\partial_t\, e_n\|_Q^2 + \tfrac{1}{2}\,(\mu\, \|\nabla_x e_n\|_{\Sigma_T}^2 + \lambda\, \|e_n\|_{\Sigma_T}^2) = \lambda\, \big(\,(f_n - \partial_t v_n + \mathrm{div}_x\, \boldsymbol{y}, e_n)_Q + (\boldsymbol{y} - \nabla_x v_n, \nabla_x e_n)_Q\big) + \mu\, \big(\,(f_n - \partial_t v_n + \mathrm{div}_x\, \boldsymbol{y}, \partial_t e_n)_Q + (\boldsymbol{y} - \nabla_x v, \nabla_x \partial_t e_n)_Q\big). \quad (15)$$

We proceed further by integrating by parts the term $(\mathbf{r}_{\mathrm{d}}, \nabla_x \partial_t e_n)_Q$:

$$\mu\, \big(\mathbf{r}_{\mathrm{d}}, \nabla_x(\partial_t e_n)\big)_Q = -\mu\, (\mathrm{div}_x(\boldsymbol{y} - \nabla_x v_n), \partial_t e_n)_Q = -\mu\, (\mathrm{div}_x \boldsymbol{y} - \Delta_x v_n, \partial_t e_n)_Q.$$

Using density arguments, i.e., $u_n \to u$, $v_n \to v \in V_{0,\underline{0}}^{\Delta_x}$, and $f_n \to f \in L^2(Q)$, for $n \to \infty$, we arrive at the identity formulated for $e = u - v$ with $u, v \in V_{0,\underline{0}}^{\Delta_x}$, i.e.,

$$\lambda\, \|\nabla_x e\|_Q^2 + \mu\, \|\partial_t\, e\|_Q^2 + \tfrac{1}{2}\,(\mu\, \|\nabla_x e\|_{\Sigma_T}^2 + \lambda\, \|e\|_{\Sigma_T}^2) = \lambda\, \big(\,(\mathbf{r}_{\mathrm{eq}}, e)_Q + (\mathbf{r}_{\mathrm{d}}, \nabla_x e)_Q\big) + \mu\, \big(\,(\mathbf{r}_{\mathrm{eq}}, \partial_t e)_Q - \mu\, (\mathrm{div}_x \mathbf{r}_{\mathrm{d}}, \partial_t e)_Q\big). \quad (16)$$

By means of the Hölder, Friedrichs, and Young inequality with positive scalar-valued parameters γ, α_1, and α_2, we deduce the estimate (13). □

The next theorem assumes higher regularity on the approximation v and $\boldsymbol{y}$.

Theorem 3. *For any $v \in V_{0,\underline{0}}^{\nabla_x \partial_t}$ and $\boldsymbol{y} \in H^{\mathrm{div}_x,1}(Q)$, we have the inequality*

$$|\!|\!| e |\!|\!|_{s,\nu_i}^2 \le \overline{\mathrm{M}}^{\mathrm{II}}(v, \boldsymbol{y}; \zeta, \beta_i, \epsilon) := \epsilon\, \mu \|\mathbf{r}_{\mathrm{d}}\|_{\Sigma_T}^2 + \zeta\, \Big(\lambda \big((1+\beta_1)\big((1+\beta_2)\, \|\mathbf{r}_{\mathrm{d}}\|_Q^2 + (1+\tfrac{1}{\beta_2}) C_{\mathrm{F}}^2\, \|\mathbf{r}_{\mathrm{eq}}\|_Q^2\big) + (1+\tfrac{1}{\beta_1})\, \tfrac{\mu^2}{\lambda^2}\, \|\partial_t \mathbf{r}_{\mathrm{d}}\|_Q^2\big) + \mu\, \|\mathbf{r}_{\mathrm{eq}}\|_Q^2\Big), \quad (17)$$

where $\nu_1 = (2 - \frac{1}{\zeta})\, \lambda$, $\nu_2 = (2 - \frac{1}{\zeta})\, \mu$, $\nu_3 = \mu\, (1 - \frac{1}{\epsilon})$, $\nu_4 = \lambda$, where C_{F} is the Friedrichs constant, $\mathbf{r}_{\mathrm{eq}}(v, y)$ and $\mathbf{r}_{\mathrm{d}}(v, y)$ are residuals in (14), $\lambda, \mu > 0$ are parameters in (6), $\zeta \in [\frac{1}{2}, +\infty)$, $\epsilon \in [1, +\infty)$, and $\beta_i > 0, i = 1, 2$.

Proof: Here, we use a different transformation of the last term in the RHS of (15):

$$\mu\, \big(\mathbf{r}_{\mathrm{d}}, \nabla_x(\partial_t e_n)\big)_Q = \mu\, (\mathbf{r}_{\mathrm{d}}, \nabla_x e_n\, n_t)_{\Sigma_T} - \mu\, (\partial_t \mathbf{r}_{\mathrm{d}}, \nabla_x e_n)_Q, \quad (18)$$

where $n_t\big|_{\Sigma_T} = 1$. Analogously to the proof of Theorem 2, we use density arguments to obtain

$$\lambda\, \|\nabla_x e\|_Q^2 + \mu\, \|\partial_t\, e\|_Q^2 + \tfrac{1}{2}\,(\mu\, \|\nabla_x e\|_{\Sigma_T}^2 + \lambda\, \|e\|_{\Sigma_T}^2) = \lambda\, \big(\,(\mathbf{r}_{\mathrm{eq}}, e)_Q + (\mathbf{r}_{\mathrm{d}}, \nabla_x e)_Q\big) + \mu\, \big((\mathbf{r}_{\mathrm{eq}}, \partial_t e)_Q\, (\mathbf{r}_{\mathrm{d}}, \nabla_x e\, n_t)_{\Sigma_T} - (\partial_t \mathbf{r}_{\mathrm{d}}, \nabla_x e)_Q\big). \quad (19)$$

Since

$$\mu\, (\mathbf{r}_{\mathrm{d}}, \nabla_x e)_{\Sigma_T} \le \tfrac{\mu}{2}\, (\tfrac{1}{\epsilon}\, \|\nabla_x e\|_{\Sigma_T}^2 + \epsilon \|\mathbf{r}_{\mathrm{d}}\|_{\Sigma_T}^2), \quad \epsilon > 0,$$

and

$$-\mu\, (\partial_t \mathbf{r}_{\mathrm{d}}, \nabla_x e)_Q \le \mu\, \|\partial_t \mathbf{r}_{\mathrm{d}}\|_Q\, \|\nabla_x e\|_Q,$$

we obtain

$$\begin{aligned}
&\lambda\, \|\nabla_x e\|_Q^2 + \mu\, \|\partial_t e\|_Q^2 + \tfrac{1}{2}\,(\lambda\, \|e\|_{\Sigma_T}^2 + \mu\, \|\nabla_x e\|_{\Sigma_T}^2) \\
&\quad \le \tfrac{\mu}{2}\, \big(\tfrac{1}{\epsilon} \|\nabla_x e\|_{\Sigma_T}^2 + \epsilon \|\mathbf{r}_{\mathrm{d}}\|_{\Sigma_T}^2\big) + \big(\lambda\, (\|\mathbf{r}_{\mathrm{d}}\|_Q + C_{\mathrm{F}}\, \|\mathbf{r}_{\mathrm{eq}}\|_Q) + \mu\, \|\partial_t \mathbf{r}_{\mathrm{d}}\|_Q\big)\, \|\nabla_x e\|_Q + \mu\, \|\mathbf{r}_{\mathrm{eq}}\|_Q\, \|\partial_t e\|_Q \\
&\quad \le \tfrac{\mu}{2}\, \big(\tfrac{1}{\epsilon} \|\nabla_x e\|_{\Sigma_T}^2 + \epsilon \|\mathbf{r}_{\mathrm{d}}\|_{\Sigma_T}^2\big) + \Big(\lambda\, \big(\|\mathbf{r}_{\mathrm{d}}\|_Q + C_{\mathrm{F}}\, \|\mathbf{r}_{\mathrm{eq}}\|_Q + \tfrac{\mu}{\lambda}\, \|\partial_t \mathbf{r}_{\mathrm{d}}\|_Q\big)^2 + \mu\, \|\mathbf{r}_{\mathrm{eq}}\|_Q^2\Big)^{1/2} (\lambda\, \|\nabla_x e\|_Q^2 + \mu\, \|\partial_t e\|_Q^2)^{1/2} \\
&\quad \le \tfrac{\mu}{2}\, \big(\tfrac{1}{\epsilon} \|\nabla_x e\|_{\Sigma_T}^2 + \epsilon \|\mathbf{r}_{\mathrm{d}}\|_{\Sigma_T}^2\big) + \tfrac{1}{2\,\zeta} (\lambda\, \|\nabla_x e\|_Q^2 + \mu\, \|\partial_t e\|_Q^2) \\
&\qquad + \tfrac{\zeta}{2}\, \Big(\lambda\, \Big((1+\beta_1)\, \big((1+\beta_2)\, \|\mathbf{r}_{\mathrm{d}}\|_Q^2 + (1+\tfrac{1}{\beta_2}) C_{\mathrm{F}}^2\, \|\mathbf{r}_{\mathrm{eq}}\|_Q^2\big) + (1+\tfrac{1}{\beta_1})\, \tfrac{\mu^2}{\lambda^2}\, \|\partial_t \mathbf{r}_{\mathrm{d}}\|_Q^2\Big) + \mu\, \|\mathbf{r}_{\mathrm{eq}}\|_Q^2\Big).
\end{aligned}$$

This estimate yields (17). □

Corollary 1 present majorants for $\lambda = 1$ and $\mu = \delta_h$, where $\delta_h = \theta\, h$, $\theta > 0$.

Corollary 1. *(i) If $v \in V_{0,\underline{0}}^{\Delta_x}$ and $\boldsymbol{y} \in H^{\mathrm{div}_x,0}(Q)$, Theorem 2 yields the estimate*

$$\|\!|e|\!\|^2_{s,\nu_i} \le \overline{\mathrm{M}}^{\mathrm{I}}_{\delta_h}(v,\boldsymbol{y};\gamma,\alpha_i) := \gamma\Big((1+\alpha_1)\,\|\mathbf{r}_{\mathrm{d}}\|^2_Q + (1+\tfrac{1}{\alpha_1})\,C_{\mathrm{F}}^2\,\|\mathbf{r}_{\mathrm{eq}}\|^2_Q + \delta_h\big((1+\alpha_2)\,\|\mathrm{div}_x\mathbf{r}_{\mathrm{d}}\|^2_Q + (1+\tfrac{1}{\alpha_2})\,\|\mathbf{r}_{\mathrm{eq}}\|^2_Q\big)\Big), \tag{20}$$

where $\nu_1 = (2-\frac{1}{\gamma})$, $\nu_2 = (2-\frac{1}{\gamma})\,\delta_h$, $\nu_3 = \delta_h$ $\nu_4 = 1$.
(ii) If $v \in V_{0,\underline{0}}^{\nabla_x\partial_t}$ and $\boldsymbol{y} \in H^{\mathrm{div}_x,1}(Q)$, then Theorem 3 yields

$$\|\!|e|\!\|^2_{s,\nu_i} \le \overline{\mathrm{M}}^{\mathrm{II}}_{\delta_h}(v,\boldsymbol{y};\zeta,\beta_i,\epsilon) := \epsilon\,\delta_h\,\|\mathbf{r}_{\mathrm{d}}\|^2_{\Sigma_T} + \zeta\Big((1+\beta_1)\big((1+\beta_2)\,\|\mathbf{r}_{\mathrm{d}}\|^2_Q + (1+\tfrac{1}{\beta_2})C_{\mathrm{F}}^2\,\|\mathbf{r}_{\mathrm{eq}}\|^2_Q\big) + (1+\tfrac{1}{\beta_1})\delta_h^2\,\|\partial_t\mathbf{r}_{\mathrm{d}}\|^2_Q + \delta_h\,\|\mathbf{r}_{\mathrm{eq}}\|^2_Q\Big), \tag{21}$$

where $\nu_1 = (2-\frac{1}{\zeta})$, $\nu_2 = (2-\frac{1}{\zeta})\,\delta_h$, $\nu_3 = \delta_h$, and $\nu_4 = 4$. In (i) and (ii), $\mathbf{r}_{\mathrm{d}}$ and $\mathbf{r}_{\mathrm{eq}}$ are defined in (14), C_{F} is the Friedrichs constant, δ_h is discretisation parameter, $\gamma,\zeta \in [\frac{1}{2},+\infty)$, $\epsilon \in [1,+\infty)$, and $\beta_i > 0, i = 1,2$.

Remark 1. For the case $\mu = 0$, the majorants presented in Theorems 2 and 3 coincide with the estimates derived in [27]. Computational properties of these estimates has been studied in [25,24]. In particular, [24] includes two benchmark examples, where error majorants are applied to v reconstructed by the space-time method. The numerical results presented there confirm the efficient performance of the majorant, i.e., ratios between majorant and error are very close to 1.

4 Numerical example

In this section, we present an example demonstrating the numerical behaviour of the derived majorants for the static case of the parabolic I-BVP. In fact, the space-time approach treats the parabolic problem as yet another elliptic problem in $\mathbb{R}^{d+1}$ with strong convection in $(d+1)$-th direction. Therefore, for the simplicity of presentation, we consider the Poisson Dirichlet problem

$$-\Delta_x u = f \quad \text{in} \quad Q := (0,1)^2 \in \mathbb{R}^2, \qquad u = 0 \quad \text{on} \quad \partial\Omega. \tag{22}$$

Let the approximation $u_h \in V_{0h}$, where $V_h \equiv \mathcal{S}_h^{p,p} := \{\hat{V}_h \circ \Phi^{-1}\}$ and $\hat{V}_h \equiv \hat{\mathcal{S}}_h^{p,p}$, be generated with NURBS of degree $p = 2$. Due to the restriction on the knots-multiplicity of $\hat{\mathcal{S}}_h^{p,p}$, we have $u_h \in C^{p-1}$.Then, $u_h(x) = u_h(x_1,...,x_d) := \sum_{i\in\mathcal{I}} \underline{u}_{h,i}\,\phi_{h,i}$, where $\underline{u}_h := \big[\underline{u}_{h,i}\big]_{i\in\mathcal{I}} \in \mathbb{R}^{|\mathcal{I}|}$ is a vector of degrees of freedom (DOFs) defined by a system

$$\mathrm{K}_h\,\underline{u}_h = \mathrm{f}_h, \quad \mathrm{K}_h := \big[(\nabla_x\phi_{h,i},\nabla_x\phi_{h,j})_Q\big]_{i,j\in\mathcal{I}}, \quad \mathrm{f}_h := \big[(f,\phi_{h,i})_Q\big]_{i\in\mathcal{I}}. \tag{23}$$

The majorant corresponding to (22) can be presented as

$$\overline{\mathrm{M}}(u_h,\boldsymbol{y}_h) := (1+\beta)\,\|\boldsymbol{y}_h - \nabla_x u\|^2_Q + (1+\tfrac{1}{\beta})\,C_{\mathrm{F}}^2\,\|\mathrm{div}_x\boldsymbol{y}_h + f\|^2_Q, \tag{24}$$

where $\beta > 0$ and $\boldsymbol{y} \in H^{\mathrm{div}_x,0}(Q)$. The approximation space for $\boldsymbol{y}_h \in Y_h \equiv \mathcal{S}_h^{q,q} := \{\hat{Y}_h \circ \Phi^{-1}\}$ is generated by the push-forward of the corresponding space $\hat{Y}_h := \hat{\mathcal{S}}_h^{q,q} \oplus \hat{\mathcal{S}}_h^{q,q}$, where $\mathcal{S}_h^{\hat{q},q}$ is the space of NURBS functions of degree q for each of two components of $\boldsymbol{y}_h = (y_h^{(1)}, y_h^{(2)})^{\mathrm{T}}$. The best estimate follows from optimisation of $\overline{\mathrm{M}}(u_h,\boldsymbol{y}_h)$ w.r.t. function $\boldsymbol{y}_h := \sum_{i\in\mathcal{I}} \underline{\mathbf{y}}_{h,i}\,\boldsymbol{\psi}_{h,i}$. Here $\boldsymbol{\psi}_{h,i}$ is the basis function generating the space Y_h, and $\underline{\mathbf{y}}_h := \big[\underline{\mathbf{y}}_{h,i}\big]_{i\in\mathcal{I}} \in \mathbb{R}^{2|\mathcal{I}|}$ is a vector of DOFs of $\boldsymbol{y}_h$ defined by a system

$$\big(C_{\mathrm{F}}^2\,\mathrm{DivDiv}_h + \beta\,\mathrm{MM}_h\big)\,\underline{\mathbf{y}}_h = -C_{\mathrm{F}}^2\,\mathrm{z}_h + \beta\,\mathrm{g}_h, \tag{25}$$

where

$$\mathrm{DivDiv_h} := \big[(\mathrm{div}_x \boldsymbol{\psi}_i, \mathrm{div}_x \boldsymbol{\psi}_j)_Q\big]_{i,j=1}^{2|\mathcal{I}|}, \qquad \mathrm{z}_h := \big[\big(f, \mathrm{div}_x \boldsymbol{\psi}_j\big)_Q\big]_{j=1}^{2|\mathcal{I}|},$$
$$\mathrm{MM_h} := \big[(\boldsymbol{\psi}_i, \boldsymbol{\psi}_j)_Q\big]_{i,j=1}^{2|\mathcal{I}|}, \qquad \mathrm{g}_h := \big[\big(\nabla_x v, \boldsymbol{\psi}_j\big)_Q\big]_{j=1}^{2|\mathcal{I}|}.$$

According to [13], the most effective results for the majorant reconstruction (with uniform refinement) is obtained, when q is set substantially higher than p. Let us assume that $q = p + m$, $m \in \mathbb{N}^+$. In the same time, when u_h is reconstructed on the mesh $\mathcal{T}_h$, we use a coarser one $\mathcal{T}_{Mh}$, $M \in \mathbb{N}^+$, to recover the flux $\boldsymbol{y}_{Mh}$.

Example 1. We consider a basic example with

$$u = (1 - x_1)\, x_1^2\, (1 - x_2)\, x_2, \qquad f = -\big(2\,(1 - 3\,x_1)\,(1 - x_2)\,x_2 - 2\,(1 - x_1)\,x_1^2\big),$$

and homogenous Dirichlet BC. For the uniform refinement test, we set $p = 2$, i.e., $u_h \in S_h^{2,2}$, and compare two different settings for the auxiliary flux: (a) $\boldsymbol{y}_h \in S_{Mh}^{q,q} \oplus S_{Mh}^{q,q}$, $q = 5$, $m = 3$, $M = 3$, and (b) $\boldsymbol{y}_h \in S_{Mh}^{q,q} \oplus S_{Mh}^{q,q}$, $q = 9$, $m = 7$, $M = 7$. The numerical results are presented in Tables 1–2, where the upper and lower parts of the tables correspond to the cases (a) and (b), respectively. The efficiency of the obtained functional majorant is confirmed by efficiency indices $I_{\mathrm{eff}}(\overline{\mathrm{M}}) = 1.1960$ (for the case (a)) and $I_{\mathrm{eff}}(\overline{\mathrm{M}}) = 1.0001$ (for the case (b)) (see the fifth column of Table 1). In the case (a), the time spent on the reconstruction of $\boldsymbol{y}_h$ (i.e., $t_{\mathrm{as}}(\boldsymbol{y}_h) + t_{\mathrm{sol}}(\boldsymbol{y}_h)$) is about $2 - 3$ times higher than the time $t_{\mathrm{as}}(u_h) + t_{\mathrm{sol}}(u_h)$. However, for the case (b), the assembling time of the systems $\mathrm{DivDiv_h}$ and $\mathrm{MM_h}$ denoted by $t_{\mathrm{as}}(\boldsymbol{y}_h)$ takes approximately 1/5-th of the assembling time for $\mathrm{K_h}$ denoted by $t_{\mathrm{as}}(u_h)$. Moreover, solving the system (25) denoted by $t_{\mathrm{sol}}(\boldsymbol{y}_h)$ requires only 1/500-th of the time spent on solving (23), i.e., $t_{\mathrm{sol}}(u_h)$.

REF	$\|\nabla_x e\|_\Omega^2$	$\overline{\mathrm{M}}$	$\overline{\mathrm{m}}_{\mathrm{d}}^2$	$\overline{\mathrm{m}}_{\mathrm{f}}^2$	$I_{\mathrm{eff}}(\overline{\mathrm{M}})$	$I_{\mathrm{eff}}(\overline{\eta})$	p
(a) $\boldsymbol{y}_h \in S_{3h}^{5,5} \oplus S_{3h}^{5,5}$ ($m = 3$, $M = 3$)							
2	1.0417e-02	1.1148e-02	1.0454e-02	3.0837e-03	1.0702	11.1821	5.0158
3	2.5648e-03	3.2802e-03	3.1548e-03	5.5723e-04	1.2789	11.0115	3.4566
4	6.3872e-04	7.8482e-04	7.6990e-04	6.6300e-05	1.2287	10.9687	2.7214
5	1.5952e-04	1.9770e-04	1.9084e-04	3.0461e-05	1.2393	10.9580	2.3602
6	3.9871e-05	4.8284e-05	4.7686e-05	2.6596e-06	1.2110	10.9553	2.1801
7	9.9672e-06	1.1974e-05	1.1921e-05	2.3575e-07	1.2013	10.9547	2.0901
8	2.4918e-06	2.9848e-06	2.9801e-06	2.0887e-08	1.1979	10.9545	2.0451
9	6.2294e-07	7.4502e-07	7.4502e-07	1.8474e-09	1.1960	10.9545	2.0225
10	1.5573e-07	1.8626e-07	1.8626e-07	1.6331e-10	1.1960	10.9545	2.0113
11	3.8934e-08	4.6564e-08	4.6564e-08	1.4547e-11	1.1960	10.9545	2.0056
(b) $\boldsymbol{y}_h \in S_{7h}^{9,9} \oplus S_{7h}^{9,9}$ ($m = 7$, $M = 7$)							
2	1.0417e-02	1.1059e-02	1.0108e-02	4.2235e-03	1.0617	11.1821	5.0158
3	2.5648e-03	2.6728e-03	2.5799e-03	4.1304e-04	1.0421	11.0115	3.4566
4	6.3872e-04	7.5593e-04	7.4667e-04	4.1181e-05	1.1835	10.9687	2.7214
5	1.5952e-04	1.7735e-04	1.6869e-04	3.8487e-05	1.1118	10.9580	2.3602
6	3.9871e-05	4.6052e-05	4.2546e-05	1.5577e-05	1.1550	10.9553	2.1801
7	9.9672e-06	1.0210e-05	1.0031e-05	7.9193e-07	1.0243	10.9547	2.0901
8	2.4918e-06	2.6188e-06	2.4946e-06	5.5197e-07	1.0510	10.9545	2.0451
9	6.2294e-07	6.3639e-07	6.2309e-07	5.9084e-08	1.0216	10.9545	2.0225
10	1.5573e-07	1.5575e-07	1.5575e-07	4.5575e-09	1.0001	10.9545	2.0113
11	3.8934e-08	3.8937e-08	3.8937e-08	4.0294e-10	1.0001	10.9545	2.0056

Table 1: Error, majorant (with its components), corresponding efficiency indices of the error estimates, and error order of convergence (e.o.c.) p w.r.t. refinement steps.

For the considered example, due to the smoothness of the exact solution, we can even use splines of the lower degree, e.g., $q = 3$, for the flux approximation, and reconstruct it on the $M = 8$ times courser mesh than for u_h. The resulting efficiency indices are illustrated in Table 4 and the corresponding times spent on approximations u_h and $\boldsymbol{y}_h$ are presented in Table 3. From Table 4, one can see the gained speed-up in the times spent on reconstruction of $\boldsymbol{y}_h$ in comparison to u_h: $\frac{t_{\mathrm{as}}(u_h)}{t_{\mathrm{as}}(\boldsymbol{y}_h)} \approx 1271$ and $\frac{t_{\mathrm{sol}}(u_h)}{t_{\mathrm{sol}}(\boldsymbol{y}_h)} \approx 46642$.

We now consider an adaptive refinement strategy, i.e., THB-Splines [14,32,8] in combination with the functional error estimate (24). We use the so-called Dörfler's marking [5] with a parameter $\theta = 0.4$. Let us start with the following setting: $u_h \in S_h^{2,2}$ is THB-Splines basis (with one level and 36 basis functions of degree 2), and $\boldsymbol{y}_h \in S_{8h}^{3,3} \oplus S_{8h}^{3,3}$ is THB-Splines basis (with one level and 81 basis functions of degree 5). We execute 12 refinement steps to obtain the error illustrated in Table 5. The time spent on the assembling, solving, and generating

REF	DOFs(u_h)	DOFs($\boldsymbol{y}_h$)	$t_{\rm as}(u_h)$	$t_{\rm as}(\boldsymbol{y}_h)$	$t_{\rm sol}(u_h)$	$t_{\rm sol}(\boldsymbol{y}_h)$	$t_{\rm e/w}(\|\nabla_x e\|)$	$t_{\rm e/w}(\overline{\rm M})$	$t_{\rm e/w}(\eta)$
(a) $\boldsymbol{y}_h \in S^{5,5}_{3h} \oplus S^{5,5}_{3h}$ ($m=3$, $M=3$)									
1	9	36	0.0009	0.0034	0.0000	0.0005	0.0001	0.0004	0.0002
2	16	36	0.0005	0.0020	0.0000	0.0006	0.0002	0.0007	0.0005
3	36	36	0.0010	0.0018	0.0000	0.0004	0.0004	0.0010	0.0022
4	100	49	0.0030	0.0092	0.0001	0.0008	0.0024	0.0038	0.0072
5	324	81	0.0099	0.0250	0.0009	0.0026	0.0159	0.0166	0.0282
6	1156	169	0.0320	0.0916	0.0051	0.0071	0.0601	0.0559	0.0982
7	4356	441	0.1180	0.3454	0.0278	0.0522	0.2270	0.2163	0.3479
8	16900	1369	0.5295	1.4091	0.2832	0.4417	0.9287	0.8324	1.5389
9	66564	4761	1.6763	5.5097	1.9016	5.3998	3.7886	3.4171	6.2132
10	264196	17689	7.3075	22.4543	20.0035	47.6661	15.0511	13.8908	24.8811
11	1052676	68121	25.6557	91.0837	141.7314	311.2439	59.9166	57.4416	98.1396
(b) $\boldsymbol{y}_h \in S^{9,9}_{7h} \oplus S^{9,9}_{7h}$ ($m=7$, $M=7$)									
1	9	100	0.0006	0.0220	0.0000	0.0039	0.0003	0.0013	0.0005
2	16	100	0.0004	0.0255	0.0000	0.0034	0.0002	0.0019	0.0008
3	36	100	0.0009	0.0285	0.0000	0.0049	0.0007	0.0024	0.0023
4	100	100	0.0020	0.0256	0.0001	0.0062	0.0018	0.0050	0.0072
5	324	100	0.0099	0.0180	0.0005	0.0058	0.0102	0.0193	0.0273
6	1156	100	0.0301	0.0157	0.0019	0.0040	0.0499	0.0584	0.0829
7	4356	100	0.0812	0.0263	0.0167	0.0045	0.1860	0.1977	0.2975
8	16900	121	0.2976	0.0698	0.2010	0.0087	0.7406	0.8024	1.1717
9	66564	169	1.2121	0.2332	1.2674	0.0146	3.0510	3.0992	4.6970
10	264196	289	4.9220	0.9035	13.7736	0.0690	12.0689	12.7465	18.7487
11	1052676	625	20.0659	3.9758	118.5357	0.3238	56.7021	59.1862	87.1078

Table 2: Assembling and solving time for systems generating DOFs of u_h and $\boldsymbol{y}_h$ as well as the time spent on element-wise (e/w) evaluation of the error, majorant, and residual error estimator w.r.t. refinements steps.

REF	$\|\nabla_x e\|^2_\Omega$	$\overline{\rm M}$	$\overline{\rm m}^2_{\rm d}$	$\overline{\rm m}^2_{\rm f}$	$I_{\rm eff}(\overline{\rm M})$	$I_{\rm eff}(\overline{\eta})$	p
2	1.0417e-02	1.1965e-02	1.0825e-02	5.0648e-03	1.1487	11.1821	5.0158
3	2.5648e-03	3.1733e-03	3.0005e-03	7.6768e-04	1.2372	11.0115	3.4566
4	6.3872e-04	9.0395e-04	8.7295e-04	1.3772e-04	1.4153	10.9687	2.7214
5	1.5952e-04	1.7571e-04	1.6338e-04	5.4779e-05	1.1015	10.9580	2.3602
6	3.9871e-05	5.1020e-05	4.9714e-05	5.8035e-06	1.2796	10.9553	2.1801
7	9.9672e-06	1.1959e-05	1.0675e-05	5.7051e-06	1.1998	10.9547	2.0901
8	2.4918e-06	2.6969e-06	2.5761e-06	5.3683e-07	1.0823	10.9545	2.0451
9	6.2294e-07	6.4308e-07	6.3365e-07	4.1905e-08	1.0323	10.9545	2.0225
10	1.5573e-07	1.6412e-07	1.5797e-07	2.7321e-08	1.0539	10.9545	2.0113
11	3.8934e-08	3.9480e-08	3.9480e-08	2.4369e-09	1.0140	10.9545	2.0056

Table 3: Error $\|\nabla_x e\|^2_\Omega$, majorant $\overline{\rm M}$ (with its components $\overline{\rm m}^2_{\rm d}$ and $\overline{\rm m}^2_{\rm f}$), and the corresponding efficiency indices of the majorant and residual error estimator.

REF	DOFs(u_h)	DOFs($\boldsymbol{y}_h$)	$t_{\rm as}(u_h)$	$t_{\rm as}(\boldsymbol{y}_h)$	$t_{\rm sol}(u_h)$	$t_{\rm sol}(\boldsymbol{y}_h)$	$t_{\rm e/w}(\|\nabla_x e\|)$	$t_{\rm e/w}(\overline{\rm M})$	$t_{\rm e/w}(\eta)$
1	9	16	0.0006	0.0009	0.0000	0.0001	0.0001	0.0002	0.0002
2	16	16	0.0006	0.0010	0.0000	0.0001	0.0002	0.0004	0.0005
3	36	16	0.0011	0.0006	0.0000	0.0001	0.0004	0.0008	0.0011
4	100	16	0.0029	0.0005	0.0001	0.0001	0.0017	0.0025	0.0054
5	324	16	0.0090	0.0005	0.0006	0.0001	0.0149	0.0130	0.0256
6	1156	16	0.0286	0.0006	0.0032	0.0001	0.0580	0.0395	0.0974
7	4356	16	0.1077	0.0007	0.0331	0.0001	0.2182	0.1285	0.3829
8	16900	16	0.3926	0.0006	0.2304	0.0001	0.8847	0.5242	1.4427
9	66564	25	1.5715	0.0014	1.6374	0.0002	3.6237	1.9630	5.8619
10	264196	49	6.3885	0.0046	16.6686	0.0004	14.3834	7.8054	22.9118
11	1052676	121	22.5053	0.0177	130.5967	0.0028	56.2099	32.5879	89.8782

Table 4: Assembling and solving time for systems generating DOFs of u_h and $\boldsymbol{y}_h$ as well as the time spent on element-wise (e/w) evaluation of the error, majorant, and residual error estimator w.r.t. refinements steps.

corresponding error estimates is illustrated in the Table 6. By using 8 times courser mesh in the refinement of the basis for $\boldsymbol{y}_h$, we have managed to spare the computational time of reconstructing the optimal $\boldsymbol{y}_h$ and speed up the over-all reconstruction of the majorant. In the current configuration, we obtain the following $\boldsymbol{y}_h$ and u_h, i.e., $\frac{t_{\rm as}(u_h)}{t_{\rm as}(\boldsymbol{y}_h)} \approx 1325$ and $\frac{t_{\rm sol}(u_h)}{t_{\rm sol}(\boldsymbol{y}_h)} \approx 4005$. The comparison of the meshes obtained for the different bulk parameters, i.e., $\theta = 0.4$ and $\theta = 0.2$, can be seen from Figure 1. It is obvious that smaller the parameter θ is taken as a bulk, more elements of the mesh will be refined.

REF	$\|\nabla_x e\|^2_\Omega$	$\overline{\mathrm{M}}$	$\overline{\mathrm{m}}^2_{\mathrm{d}}$	$\overline{\mathrm{m}}^2_{\mathrm{f}}$	$I_{\mathrm{eff}}(\overline{\mathrm{M}})$	$I_{\mathrm{eff}}(\overline{\eta})$	p
2	1.0417e-02	1.1965e-02	1.0825e-02	5.0648e-03	1.1487	11.1821	5.0158
3	7.9113e-03	8.9838e-03	8.1878e-03	3.5362e-03	1.1356	8.7164	0.9252
4	1.8426e-03	2.1299e-03	2.1137e-03	7.2176e-05	1.1559	9.6795	3.7562
5	6.1461e-04	8.8439e-04	8.3211e-04	2.3228e-04	1.4389	10.3143	4.0741
6	2.7721e-04	3.1629e-04	3.0846e-04	3.4786e-05	1.1410	9.0861	2.1188
7	1.5196e-04	1.6922e-04	1.5618e-04	5.7946e-05	1.1136	10.0945	2.0388
8	5.2273e-05	6.2761e-05	6.0891e-05	8.3085e-06	1.2006	10.0742	2.5524
9	2.7220e-05	3.5827e-05	3.4793e-05	4.5928e-06	1.3162	10.3666	1.5642
10	1.0379e-05	1.3030e-05	1.1911e-05	4.9730e-06	1.2554	10.5388	2.7512
11	5.2539e-06	5.6011e-06	5.5530e-06	2.1347e-07	1.0661	10.5762	1.5600
12	2.3568e-06	2.5967e-06	2.5018e-06	4.2137e-07	1.1018	10.7784	2.3827

Table 5: The error $\|\nabla_x e\|^2_\Omega$, majorant $\overline{\mathrm{M}}$ (with its components $\overline{\mathrm{m}}^2_{\mathrm{d}}$ and $\overline{\mathrm{m}}^2_{\mathrm{f}}$), the corresponding efficiency indices of the estimates, and e.o.c. p w.r.t. refinement steps.

REF	DOFs(u_h)	DOFs($\boldsymbol{y}_h$)	$t_{\mathrm{as}}(u_h)$	$t_{\mathrm{as}}(\boldsymbol{y}_h)$	$t_{\mathrm{sol}}(u_h)$	$t_{\mathrm{sol}}(\boldsymbol{y}_h)$	$t_{\mathrm{e/w}}(\|\nabla_x e\|)$	$t_{\mathrm{e/w}}(\overline{\mathrm{M}}))$	$t_{\mathrm{e/w}}(\eta)$
1	9	16	0.0009	0.0038	0.0000	0.0001	0.0002	0.0013	0.0011
2	16	16	0.0014	0.0042	0.0000	0.0001	0.0008	0.0020	0.0032
3	29	16	0.0058	0.0022	0.0000	0.0001	0.0130	0.0071	0.0241
4	63	16	0.0235	0.0022	0.0000	0.0001	0.0270	0.0200	0.0506
5	108	16	0.0392	0.0029	0.0001	0.0003	0.0612	0.0415	0.0969
6	229	16	0.0811	0.0022	0.0003	0.0001	0.1015	0.0837	0.1942
7	413	16	0.2114	0.0023	0.0008	0.0001	0.3056	0.2205	0.5100
8	953	16	0.6290	0.0042	0.0050	0.0001	0.7197	0.4965	1.1432
9	2195	16	0.8517	0.0028	0.0106	0.0001	1.1146	0.9008	2.0928
10	4424	16	1.9141	0.0035	0.0368	0.0001	2.9351	2.0063	4.9616
11	10590	16	3.9008	0.0029	0.1422	0.0001	5.6474	4.0477	10.1093
12	20756	25	10.6063	0.0080	0.4005	0.0001	12.2512	8.8693	21.7824

Table 6: Assembling and solving time for systems generating DOFs of u_h and $\boldsymbol{y}_h$ as well as the time spent on element-wise (e/w) evaluation of the error, majorant, and residual error estimator w.r.t. refinements steps.

Acknowledgments The research is supported by the Austrian Science Fund (FWF) through the NFN S117-03 project. Implementation was carried out using the open-source C++ library *G+smo* [23] developed at RICAM.

References

1. Y. Bazilevs, L. Beirão da Veiga, J. A. Cottrell, T. J. R. Hughes, and G. Sangalli. Isogeometric analysis: approximation, stability and error estimates for h-refined meshes. *Math. Models Methods Appl. Sci.*, 16(7):1031–1090, 2006.
2. A. Buffa and C. Giannelli. Adaptive isogeometric methods with hierarchical splines: error estimator and convergence. Technical Report arxiv: 1502.00565, arxiv:math.NA, 2015.
3. L. Dedè and H. A. F. A. Santos. B-spline goal-oriented error estimators for geometrically nonlinear rods. *Comput. Mech.*, 49(1):35–52, 2012.
4. M. R. Dörfel, B. Jüttler, and B. Simeon. Adaptive isogeometric analysis by local h-refinement with T-splines. *Comput. Methods Appl. Mech. Engrg.*, 199(5-8):264–275, 2010.
5. W. Dörfler. A convergent adaptive algorithm for Poisson's equation. *SIAM J. Numer. Anal.*, 33(3):1106–1124, 1996.
6. A. V. Gaevskaya and S. I. Repin. A posteriori error estimates for approximate solutions of linear parabolic problems. *Springer, Differential Equations*, 41(7):970–983, 2005.
7. M. Gander. 50 years of time parallel time integration. In *Multiple Shooting and Time Domain Decomposition*, volume 16, pages 69–114. Springer-Verlag, Berlin, 2015. Theory, algorithm, and applications.
8. C. Giannelli, B. Jüttler, and H. Speleers. THB-splines: the truncated basis for hierarchical splines. *Comput. Aided Geom. Design*, 29(7):485–498, 2012.
9. P. Hansbo. Space-time oriented streamline diffusion methods for nonlinear conservation laws in one dimension. *Comm. Numer. Meth. Eng.*, 10(3):203–215, 1994.
10. K.A. Johannessen. An adaptive isogeometric finite element analysis. Technical report, Master's thesis, Norwegian University of Science and Technology, 2009.
11. C. Johnson. *Numerical solution of partial differential equations by the finite element method.* Dover Publications, Inc., Mineola, NY, 1987.
12. C. Johnson and J. Saranen. Streamline diffusion methods for the incompressible euler and navier-stokes equations. *Math. Comp.*, 47(175):1–18, 1986.
13. S. K. Kleiss and S. K. Tomar. Guaranteed and sharp a posteriori error estimates in isogeometric analysis. *Comput. Math. Appl.*, 70(3):167–190, 2015.

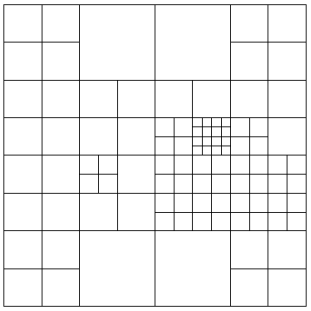

REF 4

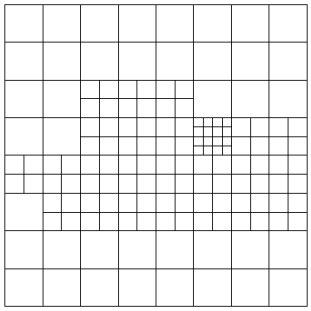

REF 4

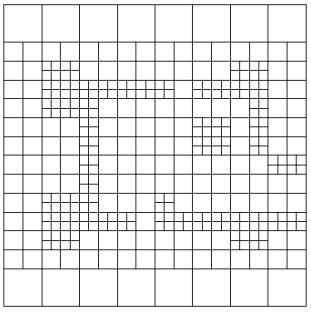

REF 6

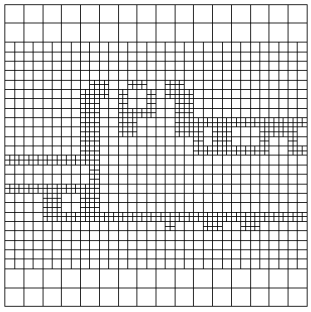

REF 6

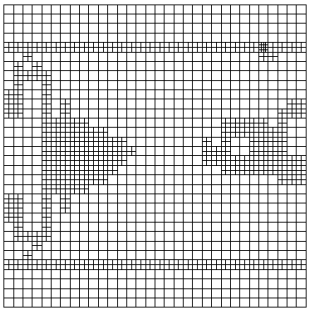

REF 8

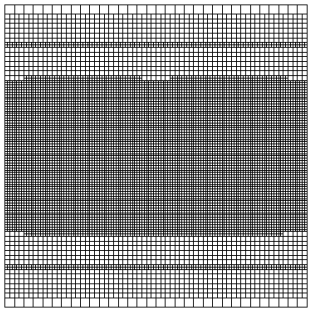

REF 8

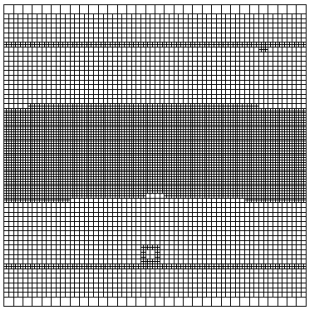

REF 10

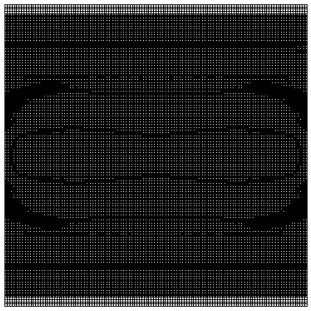

REF 10

Fig. 1: Adaptive meshes obtained for the bulk parameters $\theta = 0.4$ (left) and $\theta = 0.2$ (right).

14. R. Kraft. Adaptive and linearly independent multilevel B-splines. In *Surface fitting and multiresolution methods (Chamonix–Mont-Blanc, 1996)*, pages 209–218. Vanderbilt Univ. Press, Nashville, TN, 1997.
15. M. Kumar, T. Kvamsdal, and K. A. Johannessen. Simple a posteriori error estimators in adaptive isogeometric analysis. *Comput. Math. Appl.*, 70(7):1555–1582, 2015.
16. G. Kuru. Goal-adaptive isogeometric analysis with hierarchical splines. Technical report, Master's thesis, Mechanical Engineering, Eindhoven University of Technology, 2013.
17. G. Kuru, C. V. Verhoosel, K. G. van der Zee, and E. H. van Brummelen. Goal-adaptive isogeometric analysis with hierarchical splines. *Comput. Methods Appl. Mech. Engrg.*, 270:270–292, 2014.
18. O. A. Ladyzhenskaya. On solvability of classical boundary value problems for equations of parabolic and hyperbolic types. *Dokl. Akad. Nauk SSSR*, 97(3):395–398, 1954.
19. O. A. Ladyzhenskaya. *The boundary value problems of mathematical physics*. Springer, New York, 1985.
20. U. Langer, S. Matculevich, and S. Repin. A posteriori error estimates for space-time iga approximations to parabolic initial boundary value problems. *arXiv.org*, math.NA/1612.08998, 2016.
21. U. Langer, S. Moore, and M. Neumüller. Space-time isogeometric analysis of parabolic evolution equations. *Comput. Methods Appl. Mech. Engrg.*, 306:342–363, 2016.
22. O. Mali, P. Neittaanmäki, and S. Repin. *Accuracy verification methods*, volume 32 of *Computational Methods in Applied Sciences*. Springer, Dordrecht, 2014.
23. Angelos Mantzaflaris, ..., and others (see website). G+smo (geometry plus simulation modules) v0.8.1. http://gs.jku.at/gismo, 2015.
24. S. Matculevich. *Fully reliable a posteriori error control for evolutionary problems*. PhD thesis, Jyväskylä Studies in Computing, University of Jyväskylä, 2015.
25. S. Matculevich and S. Repin. Computable estimates of the distance to the exact solution of the evolutionary reaction-diffusion equation. *Appl. Math. and Comput.*, 247:329–347, 2014.
26. S. Repin. *A posteriori estimates for partial differential equations*, volume 4 of *Radon Series on Computational and Applied Mathematics*. Walter de Gruyter GmbH & Co. KG, Berlin, 2008.
27. S. I. Repin. Estimates of deviations from exact solutions of initial-boundary value problem for the heat equation. *Rend. Mat. Acc. Lincei*, 13(9):121–133, 2002.
28. S.I. Repin. A posteriori error estimation for nonlinear variational problems by duality theory. *Zapiski Nauchnych Seminarov POMIs*, 243:201–214,, 1997.
29. S.I. Repin. A posteriori error estimates for approximate solutions to variational problems with strongly convex functionals. *Journal of Mathematical Sciences*, 97:4311–4328, 1999.
30. A. Tagliabue, L. Dedè, and A. Quarteroni. Isogeometric analysis and error estimates for high order partial differential equations in fluid dynamics. *Comput. & Fluids*, 102:277–303, 2014.
31. K. G. van der Zee and C. V. Verhoosel. Isogeometric analysis-based goal-oriented error estimation for free-boundary problems. *Finite Elem. Anal. Des.*, 47(6):600–609, 2011.
32. A.-V. Vuong, C. Giannelli, B. Jüttler, and B. Simeon. A hierarchical approach to adaptive local refinement in isogeometric analysis. *Comput. Methods Appl. Mech. Engrg.*, 200(49-52):3554–3567, 2011.
33. P. Wang, J. Xu, J. Deng, and F. Chen. Adaptive isogeometric analysis using rational pht-splines. *Computer-Aided Design*, 43(11):1438–1448, 2011.
34. E. Zeidler. *Nonlinear functional analysis and its applications. II/A*. Springer-Verlag, New York, 1990.